



# Development, QbD based optimization and *in vitro* characterization of Diacerein loaded nanostructured lipid carriers for topical applications

Disha Kesharwani<sup>a</sup>, Swarnali Das Paul<sup>b,\*</sup>, Rishi Paliwal<sup>c</sup>, Trilochan Satapathy<sup>d</sup>

<sup>a</sup> Columbia Institute of Pharmacy, Raipur, Chhattisgarh, India

<sup>b</sup> Shri Shankaracharya College of Pharmaceutical Sciences, Bhilai, 490 020, C.G, India

<sup>c</sup> IGNTU, Amarkantak, Madhya Pradesh, India

<sup>d</sup> University College of Pharmacy, Chhattisgarh Swami Vivekanand Technical University Bhilai, Durg, Chhattisgarh, India

## ARTICLE INFO

### Keywords:

DCN  
Nanostructured lipid carrier  
Central Composite Design  
Topical application  
Gels  
TEM  
Entrapment efficiency

## ABSTRACT

**Objective:** DCN is a chondro-protective agent which displays inadequate oral bioavailability along with gastrointestinal side effects. It is a choice of drug for treatment of osteoarthritis. Therefore, the objective of this study was to develop and optimize DCN loaded nanostructured lipid carrier (NLCs) for topical delivery.

**Method:** NLCs were prepared by hot homogenization followed by sonication method. The formulation was optimized by 2 factor 3 level central composite design taking two independent variables i.e. concentration of stearic acid (A) and concentration of oleic acid (B), and three independent variables, particles size (Y1), % entrapment efficiency (Y2) and % drug release at 24 hours (Y3).

**Result:** The particle size, % entrapment efficiency and *in-vitro* drug release at 24 hours of optimized formulation was found 173.76 nm, 91.30%, and 94.17% respectively. The optimized DCN-NLC formulations were analyzed by DSC and XRD, TEM, and FTIR studies. DCN-NLC loaded gel was prepared and characterized for physical examination, viscosity and stability parameters. DCN-NLC in the gel form displayed sustained drug release and significant ( $p < 0.05$ ) tissue penetration *in vitro* in comparison to plain gel and DCN solution. The drug release kinetics study illustrated the Higuchi's release pattern for prolonged period of time. *Ex vivo* permeation study result supported good topical penetration for DCN using DCN-NLCs.

**Conclusion:** Conclusively, the developed formulation has potential for topical application for future pre-clinical studies.

## 1. Introduction

Diacerein (DCN), an anti-osteoarthritic agent, is a di-acetylated derivative of rhein and a chondroprotective agent (Nguyen et al., 1994). It belongs to the analgesic, antipyretic and anti-inflammatory categories. Rhein is composed of an anthraquinone ring and is the active metabolite of DCN (Khandavilli & Panchagnula, 2007). These molecules inhibit the production of interleukin-1 $\beta$  and down-regulate interleukin 12 and tumor necrosis factor  $\alpha$  which are key mediators for the production and maintenance of inflammation. Several studies proved that these mediators can be inviting therapeutic targets (Pelletier et al., 2339). Based on these facts, DCN can be used as a promising candidate in the management of osteoarthritis (Pelletier et al., 2339).

Due to its low aqueous solubility and high permeability, DCN falls under biopharmaceutical class II. It has molecular weight 368.2 g/mol

and is practically insoluble in water. It possesses a pKa value of about  $3.01 \pm 0.20$ . Due to its poor solubility and other poor physicochemical properties, its oral formulations have not been successful. Additionally, its oral administration precipitates severe gastrointestinal adverse effects too. Patients on oral dose of DCN are noncompliant with its 40–50 mg twice daily regimen for long treatment periods. Such unavoidable side effects of oral DCN cause a cutoff of regular regimens and even some countries have prohibited the use of DCN (Giannellini et al., 2005). Since DCN possesses eminent properties to treat the disease, it can't be dropped away on the cost of only associated side effects. Novel drug delivery approaches for DCN are needed for the treatment of osteoarthritis.

In the past few years, the use of topical drug carriers has been enhanced drastically. These carriers modify the drug permeation through the skin to a greater extent by the use of permeation enhancers.

\* Corresponding author.

E-mail address: [swarnali34@gmail.com](mailto:swarnali34@gmail.com) (S. Das Paul).

<https://doi.org/10.1016/j.jrras.2023.100565>

Received 20 December 2022; Received in revised form 10 March 2023; Accepted 16 March 2023

Available online 1 April 2023

1687-8507/© 2023 Published by Elsevier B.V. on behalf of The Egyptian Society of Radiation Sciences and Applications. This is an open access article under the CC BY-NC-ND license (<http://creativecommons.org/licenses/by-nc-nd/4.0/>).

However, chemical enhancers may be harmful in chronic application cases (Aliaa et al., 2011). Formulation scientists are developing topical drug delivery system without the use of chemical enhancers. One of the well known techniques for resolving this task is the development of a lipid-based nano-carrier system (Gupta et al., 2005). Over the past few years, nanostructured lipid carrier system (NLCs) has gathered pronounced importance as lipid carrier for topical delivery of therapeutics. These systems have shown more versatility and uniqueness in terms of permeability, stability, and drug release as compared to liposomes, polymeric nanoparticles, and solid lipid nanoparticles etc (Liu et al., 2009).

NLCs are the advanced generation to solid lipid nanoparticles (SLNs) as they are composed of both solid and liquid lipids. Further, NLCs provide better drug loading, drug release, and stability as compared to SLNs (Paliwal et al., 2020). The liquid lipid provides greater solubility than the solid lipid content, and this leads to greater entrapment efficiency. Also, the unique lipid composition of NLCs ensures the greater contact of the drug with the stratum corneum (Rai et al., 2008). The nanoparticle size of NLCs enhances the drug flux inside the skin. Both of the above-mentioned properties collectively make the NLCs as one of best alternatives for topical administration (Kesharwani et al., 2019; Tiwari et al., 2014).

In recent times as per ICH guidelines Q8, various statistical experimental designs have been utilized for optimization. These designs are more proficient than the usual trial and error methods along with a lesser number of trials (Schwartz et al., 2007). These methods are time and cost-efficient. These designs also provide information about the interaction between the variables (Jain et al., 2015). The response surface designs are one of the best designs used for optimization (Zhang et al., 2004). The objective of the present experimental work was to develop and optimization of nanostructured lipid carriers of DCN using design expert software version 11. The optimization involves various characteristic parameters including particle size, surface morphology, entrapment efficiency, in-vitro drug permeation study, and stability study.

## 2. Experimental methods

### 2.1. Materials

DCN was purchased from Quingdao Sigma Co. Ltd. China. The other chemicals used in this study such as ethanol, methanol, disodium hydrogen orthophosphate, potassium di-hydrogen orthophosphate, stearic acid, oleic acid, Tween 80, and Carbopol 940 were purchased from Loba Chemicals Mumbai, India.

### 2.2. Methods

#### 2.2.1. QTTP identification

According to International Conference on Harmonization (ICH) Q8 guidelines, a quality target product profile (QTTP) should be identified before starting the experiment. The QTTP consists of sets of essential features or targets related to the quality, safety, and efficacy of the pharmaceutical products. For the selected carrier i.e. NLC, the QTTPs are mentioned in Table 1.

#### 2.2.2. Design of experiments

Face centered Central Composite Design (CCD) (Design-Expert version 11) with 8 axial and 05 centre points was chosen for the DCN-loaded NLCs formulation. Two factors, namely the concentration of stearic acid (A) and concentration of oleic acid (B) were selected to determine their effects on three responses i.e., particle size of the NLCs (Y1), %entrapment efficiency (Y2), and in-vitro drug release at 24 h (Y3). Accordingly, 13 preliminary-formulations of different combinations were prepared in random order as shown in Table 2.

**Table 1**

Quality target product profile.

S. No.	QTTP Elements	Target	Justification
1.	Dosage form	Gel	–
2.	Route of administration	Topical (Semisolid)	Eliminates
3.	Dosage strength	10 mg	Decreased dose with enhanced effect
4.	Particle size range	<200 nm	Causes easy penetration through the skin
5.	% Entrapment efficiency	75%	Greater the drug entrapment, lower the total volume/ excipient for administration
6.	% Drug permeation in 24 h	75%	Higher drug permeation provides greater bioavailability
7.	Surface morphology	Smooth and spherical	–
8.	Stability	A minimum of 6 months stability at room temperature	Assures the quality of product
9.	pH	6.4–7	For avoiding skin irritation

### 2.3. Preparation of DCN loaded nanostructured lipid carries (DCN-NLCs)

The hot homogenization method was used for the preparation of DCN-loaded NLCs. Stearic acid and oleic acid were taken in the proportion of about 20–60%. Lipids were melted at 80 °C and the drug was incorporated into the melted lipid. An aqueous solution containing tween 80 and gelucire 44/14 was prepared and its temperature was also maintained at 80 °C. The hot melted lipid mixture was then added dropwise to the surfactant solution under homogenization at the rate of 4000 rpm for 1 h to obtain the primary emulsion. Then the primary emulsion was homogenized well and sonicated using a probe sonicator (Model 0) for 10 min to obtain the NLCs. The prepared formulation was stored at 4 °C (Mira et al., 2010; Tran et al., 2014).

### 2.4. Preparation of gel

The final gel was prepared incorporating an optimized NLC formulation as suggested by design of the experiment. It was prepared by dispersing different concentrations of Carbopol 940 in freshly prepared NLCs formulation and subsequently neutralizing the Carbopol dispersion by the addition of triethanolamine. The final concentration chosen was 0.5% (Naglakshmi et al., 2018).

### 2.5. Characterization

#### 2.5.1. Particle size analysis

The particle size and polydispersity index (PDI) of the prepared formulations were analyzed by using the Litesizer 500 (Anton Paar) at 25 °C and backscattered angle (Nimila et al., 2010; Patel et al., 2014).

#### 2.5.2. Determination of entrapment efficiency (%EE) and drug loading (DL)

For the determination of % EE and DL, a refrigerated centrifuge (C-12 Remi instruments, India) was used. The instrument was operated at 15,000 rpm for 30 min at 4 °C. After that, the un-entrapped drug-containing supernatant was separated from the NLCs. The free drug concentration was measured by measuring the absorbance at 257 nm with a UV-Visible spectrophotometer (Shimadzu, Japan). The % EE and DL were calculated using the given formulas. This procedure was repeated thrice<sup>17,18</sup>.

$$\%EE = \frac{[\text{Total drug} - \text{Free drug}]}{(\text{Total drug})} \times 100$$

$$\%DL = \frac{[\text{Initial drug} - \text{Free drug}]}{(\text{Mixed lipid})} \times 100$$

**Table 2**  
Formulation table for preliminary experimental batches (CCD).

Trial Number	Drug (mg)	Concentration of stearic acid (A)		Concentration of oleic acid (B)		Tween 80 (ml)	Gelucire 44/14 (mg)	Water (q s upto 100 mL)
		Coded Factor Levels	Original Values (mg)	Coded Factor Levels	Original Values (mg)			
1	10	-1	200	-1	0.47	1	15	100
2	10	+1	600	-1	0.47	1	15	100
3	10	-1	200	+1	0.94	1	15	100
4	10	+1	600	+1	0.94	1	15	100
5	10	-1	200	0	0.70	1	15	100
6	10	+1	600	0	0.70	1	15	100
7	10	0	400	-1	0.47	1	15	100
8	10	0	400	+1	0.94	1	15	100
9	10	0	400	0	0.70	1	15	100
10	10	0	400	0	0.70	1	15	100
11	10	0	400	0	0.70	1	15	100
12	10	0	400	0	0.70	1	15	100
13	10	0	400	0	0.70	1	15	100

### 2.5.3. In-vitro drug release study

Franz diffusion cell was used to evaluate the drug release from the prepared formulation. For this study dialysis membrane, 70 (Pore size 2.4 nm and molecular weight cut off between 12,000 and 14,000) was used. The assembly was set up by fitting the membrane on the Franz diffusion cell having a surface area of about 2.68 cm<sup>2</sup>. NLC dispersion (equivalent to 1 mg of DCN) was filled in the donor compartment and the receptor medium was phosphate buffer pH 6.8. The capacity of the receptor compartment was about 100 mL. The whole assembly was mounted on a magnetic stirrer at 700 rpm. The temperature was maintained at 37 ± 0.5 °C during the experiment. The samples were withdrawn and the sink condition was maintained from time to time. The samples were analyzed at 257 nm by the UV-Visible spectrophotometer. This study was followed for all the preliminary formulations, optimized DCN-NLCs gel, DCN loaded gel, and plain DCN dispersion (Agrawal et al., 2021).

## 2.6. Evaluation of optimized formulation

### 2.6.1. Drug release kinetics

The amount of DCN from NLC gel was permeated through the dialysis membrane. To explain the release kinetics, mathematical models i.e. zero order, first order, and Higuchi's models were used. The data obtained were plotted for the above-mentioned kinetic models. For zero-order cumulative percentage drug remaining versus time (eq.), for first-order log cumulative %, drug release versus time and for Higuchi's model cumulative % drug release versus square root of time were plotted. The goodness of fit test was applied for selecting the most suitable model for release kinetics (Roberts et al., 1997).

### 2.6.2. Ex-vivo drug permeation study

For studying the permeability of DCN-NLCs formulation, healthy albino rats were selected. The abdominal part of albino rats of weight approximately 150 ± 5 gm was properly shaved and subcutaneous skin was removed surgically. The extra fat was removed by using isopropyl alcohol. Franz diffusion cell was assembled with fresh hairless full thickness rat skin. The total surface area was about 2.68 cm<sup>2</sup>. The stratum corneum of the skin facing the donor compartment was filled with the NLC dispersion. The receptor compartment was filled with phosphate buffer pH 6.8. The capacity of the receptor compartment was 10 mL. This assembly was placed over a magnetic stirrer at 700 rpm and a thermostat was maintained at 37 ± 0.5 °C throughout the experiment. Samples were withdrawn from the receptor compartment at different time intervals and analyzed by UV spectrophotometer at 257 nm. The sink condition was maintained by immediately adding a fresh buffer solution. A similar study was carried out with plain DCN dispersion (Lunter & Daniels, 2013).

### 2.6.3. Fourier transforms infrared spectroscopy (FTIR)

Shimadzu FT-IR spectrophotometer was used for determining the drug's identity and the compatibility of the drug with other ingredients used for the preparation of NLC by using KBr discs. A scanning speed of 2 mm/s was used with a resolution of 4 cm<sup>-1</sup>. The region selected for the run was 4000–400 cm<sup>-1</sup>. The dry air purge condition was maintained in the instrument throughout the analysis (Agrawal et al., 2021).

### 2.6.4. X-ray diffraction (XRD)

X-ray diffraction is a quick analytical technique generally used for the identification of a crystalline phase of the material. The pure drug DCN and the optimized lyophilized NLC samples were analyzed for XRD patterns by PAN analytical 3 kW X'pert Powder Multifunctional. The equipment was fitted with Cu LFF high-resolution X-ray. A 2θ angle scale from 10 to 60° range was chosen for scanning (Souto et al., 2006).

### 2.6.5. Differential scanning calorimetry (DSC)

Differential scanning calorimetry studies for the pure drug, physical mixture, and the optimized lyophilized NLCs formulations were carried out. This method is an analytical method for determining the thermal properties and recrystallization behavior of the material. Before the analysis, the instrument was calibrated with standard Indium for achieving accurate results. A heating rate of 10 °C/min was employed at a range of 0–300 °C. A continuous nitrogen purge was applied during the whole study (Wavikar and Vavia, 2015).

### 2.6.6. Surface morphology study by HRTEM

The surface morphology of the optimized formulation was done by high-resolution transmission electron microscopy (HRTEM). The sample was visualized by dropping it on a carbon-coated copper grid. The sample was stained negatively with phosphotungstic acid and the extra sample was removed using Whatman filter paper. The sample was observed under the microscope after drying (Agrawal et al., 2021).

## 2.7. Evaluation of the DCN-NLCs based gels

### 2.7.1. Physical investigations

The optimized gel was evaluated for various organoleptic properties (color, odor, phase separation, etc.) along with their grittiness, and greasiness. For the determination of the homogeneity of the prepared gel, 100 mg of gel was pressed between the thumb and the index finger, and the presence of any gritty particles was noticed. Another parameter of washability of prepared gel was also determined by 100 mg of the gel rubbed on the back skin of the hand and then washing with water for checking whether it is washable or not. The pH of the gel was measured by a digital pH meter (HI 96107 pHep, HANNA instruments). For this test, 1 g of gel was diluted with 9 g of double-distilled water. All the above tests were performed in triplicates (Naglakshmi et al., 2018).

2.7.2. Determination of spreadability of DCN-NLCs gel

For the determination of spreadability, the parallel plate method was selected. A glass plate was taken and a circle of 1 cm diameter was marked on it. Subsequently, 0.1 gm gel was weighed and placed on that circle. The gel was covered with another glass plate and a weight of 200 gm was put on the glass plate for 5 min. The increase in diameter was noted (Naglakshmi et al., 2018).

2.7.3. Measurement of viscosity of DCN-NLCs gel

The determination of the viscosity of the prepared gel was carried out with a Brookfield viscometer using spindle 7 at different angular velocities at a temperature of 37 °C ± 1 °C (Naglakshmi et al., 2018).

2.7.4. Stability study

The final formulation was taken for accelerated stability study as per the ICH guidelines Q1A, to evaluate any kind of changes physically or chemically on storage. For this study, all the formulations were kept in three different conditions. The first one was at refrigerated temperature (4±2 °C) and the second one was at 25±2 °C/60 ± 5% RH and the third one was an accelerated study at 40 ± 2 °C temperature and 75 ± 5% RH for 90 days. After the study, the formulations were analyzed for various evaluation parameters selected (Gupta et al., 2014; Jadon et al., 2009).

2.8. Statistical analysis

In this study, student’s t-test was used for comparison of two groups while for multiple group comparison ANOVA followed by post-hoc test were applied. A p value less than 0.05 was considered significant in all cases.

3. Result and discussion

3.1. Optimization through DOE

A face centered central composite design with two factors at 3 different levels was selected to study the effects on three response variables. The two variables were the concentration of stearic acid (A) and the concentration of oleic acid (B). The independent variables were screened through a central composite design and 13 different formulation concentrations were obtained as shown in Table 2. Out of these 13 runs, there were 8 axial points and 5 centre points. Three different response variables chosen were particle size (Y<sub>1</sub>), % entrapment efficiency (Y<sub>2</sub>), and % drug release at 24 h (Y<sub>3</sub>). The proto-formulations were studied for the above-selected response parameters and the obtained results were modeled on design for obtaining an analysis of variance, various equations, and graphs. The selected three response variables are the most critical response variables that are required to be discussed for maintaining the quality of the formulation. The modeling of responses in experimental design was shown in Table 3. Also, the mathematical modeling was accomplished by equation (1) (2), and (3) for responses Y<sub>1</sub>, Y<sub>2</sub>, and Y<sub>3</sub> respectively to attain the first-order polynomial equation based on significant influences among two factors (A and B) of the design.

3.1.1. Effect of the independent variables on particle size (Y<sub>1</sub>)

In order to establish a connection between various independent and response variables particle sizes of prepared NLCs and different mathematical models were analyzed for the test of fit using the design expert software V 11. The quadratic model was found to fit with the significant p-value (<0.05) and non-significant lack of fit value of 0.1267. Also, the model F value of 1185.85 implies that it is significant for the chosen response variables. The difference between the adjusted and predicted R<sup>2</sup> value is less than 0.2 which provides the information of reasonable agreement between the two. Table 3 shows the particle size results of different NLCs prepared. The size of all 13 proto-formulations ranges from 174.5 nm to 277.9 nm. The polynomial equation obtained for the

Table 3

Modeling of responses in Experimental Design for DCN-NLCs.

Formulations	Concentration of Stearic acid (mg)	Concentration of Oleic Acid (mg)	Particle Size (nm)	% EE	In-vitro Drug release at 24 h (%)
F1	0.2	0.47	168.5	91.3	94.17
F2	0.6	0.47	235.8	91.1	83.63
F3	0.2	0.94	228.6	84.3	84.86
F4	0.6	0.94	279.5	91.2	86.23
F5	0.2	0.70	210.9	88.7	88.21
F6	0.6	0.70	272.9	92.0	84.10
F7	0.4	0.47	180.3	85.6	89.99
F8	0.4	0.94	228.6	82.1	87.47
F9	0.4	0.70	219.7	84.7	88.67
F10	0.4	0.70	219.7	84.4	88.67
F11	0.4	0.70	219.7	84.4	88.67
F12	0.4	0.70	219.4	84.3	88.84
F13	0.4	0.70	219.7	86.1	88.67

particle size of the prepared formulation is given in equation (1).

$$\text{Particle Size} = 219.79 + 30.03A + 25.35B + 4.10 AB + 22.72 A^2 - 14.73B^2 \dots \dots \dots (1)$$

These coefficients in the equation explain the size and direction of the relationship between the variables. The polynomial equation obtained for particle size clearly shows that both the factors (A and B) positively affect the response variable i.e. the increase in the concentration of solid and liquid lipids increases the particle size of the formulations. As the coefficient of factor A is greater than factor B, it is clear that the concentration of solid lipid has a greater impact on particle size as compared to liquid lipid. The relationship between both the variables was further described by using three-dimensional response graphs as shown in Fig. 1[A]. It is visible from the 3D plot that the particle size increases significantly with the increase in lipid concentration. Initially, when the solid lipid is increased to level 0, there is a slender increase in particle size. After that, the increase is brisk. This increase in particle size can be explained in terms of the coalescence behavior of lipids at high concentrations. When the concentration of solid lipid increases, the viscosity of NLC dispersion also increases. The increase in viscosity of dispersion causes an increase in surface tension followed by higher particle size. The particle size was slightly decreased when the liquid lipid is incorporated in higher concentrations. (i.e. in +1 region of factor B). The above results are in agreement with the previously published literatures (Alsarra et al., 2005; Nimila et al., 2010; Patel et al., 2014).

The smallest particle sizes were obtained at lower concentrations of solids as shown in 3D plots. From the study, it is clear that lipid concentration is a vital factor in the case of drug loading also. It is greatly influenced by lipid concentration and drug to lipid ratio in NLCs. For increasing the drug loading a drug concentration is required. This statement can be justified by the fact that a higher concentration of the drug is required to saturate the lipid mixture as low concentrations of drugs cannot achieve saturation (Nimila et al., 2010; Patel et al., 2014).

3.1.2. Effect of independent factors on % entrapment efficiency (Y<sub>2</sub>)

The % EE of DCN-NLCs was observed and found in the range of 82.1% for F8 to 91.3% for F1. A relation between the factor variable and % EE was established with the help of used software. Again in the case of % EE, quadratic model fit was significant with a p-value <0.05, and lack of fit was found not significant with a value of 0.9998. Model F-value of 85.46 indicates that it is significant for the chosen response variables. The predicted and adjusted R<sup>2</sup> values are in reasonable agreement with each other. The adequate precision provides an adequate signal.

The quadratic equation found for %EE is given below

$$\%EE = +84.77 + 1.67A - 1.73B + 1.78AB + 5.60A^2 - 0.9034 B^2 \dots \dots \dots (2)$$

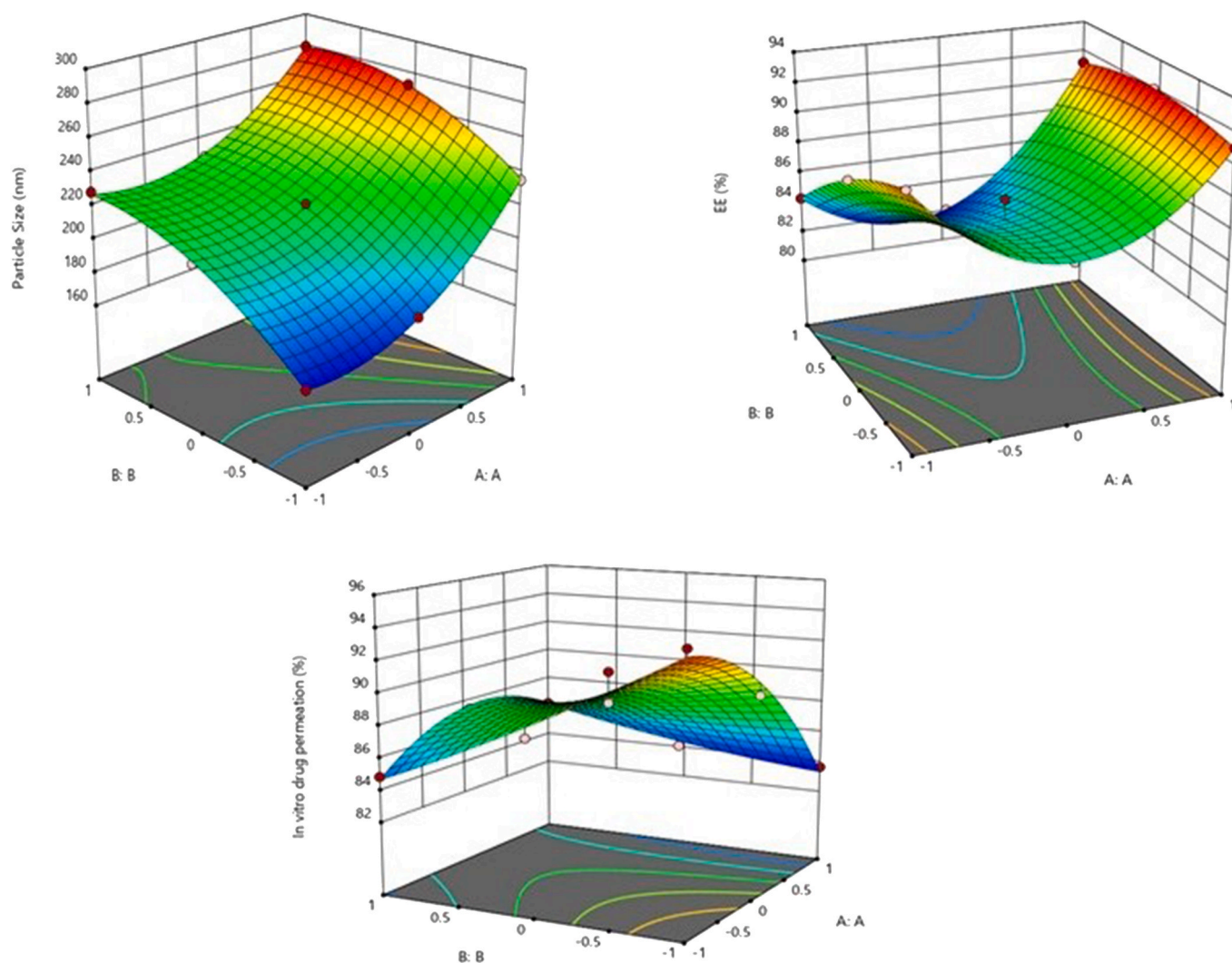


Fig. 1. 3D Response surface curve for different parameters [A] Particle size; [B] % Entrapment efficiency; [C] % Drug release.

The equation clearly explains that the % EE is directly proportional to factor A i.e. concentration of solid lipid while it is inversely proportional to the concentration of liquid lipid. It is also clear from the coefficients that factor B is more influential as compared to factor A. The 3D curve in Fig. 1[B] shows that % EE is higher at the  $-1$  level of factor A; it decreases with a slight increase in the concentration of stearic acid. After that, it increases gradually with an increase in solid lipid concentration. On the other hand, there is a negative effect of liquid lipid on %EE. It decreases with an increase in LL concentration. The highest % EE was achieved with  $+1$  level of stearic acid and  $0$  levels of oleic acid. This type of behavior might be due to the initial increase in insolubilization of the drug in solid lipid matrix (Alsarra et al., 2005; Nimila et al., 2010; Patel et al., 2014).

### 3.1.3. Effect of independent factors on % drug release at 24 h ( $Y_3$ )

The % drug release was determined for all the formulations and found in the range of 83.63%–94.17% for F2 and F1 respectively. A significant correlation can be observed between the independent and dependent variables as shown by the statistics shown by the software. For this response, the quadratic model was found to fit with a significant p-value of less than  $<0.05$  and a non-significant lack of fit value of 0.5758. F value of 27.26 approves the significance of the model.

The polynomial equation obtained for the % drug release is given in equation (3).

$$\% \text{ drug release} = +88.91 - 2.21A - 1.54A + 2.98AB - 2.25A^2 + 0.321B^2 \dots \dots (3)$$

This equation clearly explains that both factors A and B negatively affect the response variables. The increase in the concentration of solid and liquid lipids decreases the %drug release rate. If we compare the lipids, the solid lipid is more influential than the liquid lipid. The response surface plots (Fig. 1[C]) show that there is a gradual decrease in response with an increase of factor A while in the case of factor B the response increases slightly from a level of  $-1$  to  $0$  after that a sharp decrease was notified (Alsarra et al., 2005; Nimila et al., 2010; Patel et al., 2014). Validation of all the polynomial equations was done by ANOVA mentioned in Table 4.

### 3.2. Validation by point prediction

After completion of prior statistical parameters including an illustration of the effect of various independent factors on responses, the numerical optimization section of the software provides validation of all results by point prediction. This section provides selected formulation variables value in the form of checkpoint formulations to achieve the goal of the selected responses. For obtaining these formulations constraints were set. For response 1, it was set to minimum value whereas, for responses 2 and 3, the constraints were set to maximum values. The software gave the checkpoint formulations with a desirability function. The formulation with maximum desirability value was selected with a

**Table 4**  
Summary of ANOVA for responses.

Fit Parameter	p- value			Interpretation
	Particle Size	%Entrapment efficiency	% Drug permeation rate	
Model	<0.0001	<0.0001	0.0002	significant
R <sup>2</sup>	0.9988	0.9839	0.9512	–
R <sup>2</sup> Adjusted	0.9980	0.9724	0.9163	–
Lack of Fit	0.1267	0.9998	0.5758	not significant
A	<0.0001	0.0002	0.0003	significant
B	<0.0001	0.0001	0.0027	significant
AB	0.0005	0.0004	0.0002	significant
A <sup>2</sup>	<0.0001	<0.0001	0.0028	significant
B <sup>2</sup>	<0.0001	0.0336	0.5400	not significant

factor A value of 0.917 and factor B value of 0.913. For this combination of variables, the responses predicted by the software were noted as the particle size of 172.49 nm, % EE of 90.26%, and in vitro drug release rate of 93.20%. This formulation was prepared and evaluated for different evaluation parameters. An overlay plot is given in Fig. 2. The yellow and grey regions can be seen in this plot. The yellow region indicates the area where all the criteria are satisfied. This yellow area is known as the sweet spot. The optimized formulation falls under this area. Table 5 shows the detail of the optimized formulation.

### 3.3. Evaluation of optimized formulation

#### 3.3.1. Drug release and release kinetics study

The in vitro drug release study was performed for optimized NLCs dispersion, optimized NLCs loaded gel, plain DCNs dispersion, and plain DCNs gel respectively. A comparative table and graph for the cumulative % drug release study of the above-mentioned formulations are given in Table 6 and Fig. 3 respectively. The NLC dispersion displayed 94.17% drug release at 24 h. While NLCs loaded gel released 90.28% of the drug at 24 h in a more sustained manner. This sustained release of the drug can be attributed to the appropriate arrangement of solid and liquid

lipids. This sustained release was slowed down by the cross-linking of polymer molecules in the gel. Whereas in the case of plain DCNs dispersion, an immediate burst release of 44.64% was found in 1st hour. This release rate was almost 5.5 times higher than NLC dispersion. At 2 h drug release from plain dispersion was 86.07% and at the end of 4 h, the release rate was found to be constant at 87%.

When we incorporated the DCN dispersion into a gel the release became a little bit slow as compared to plain dispersion. In the first hour, 38.14% of the drug was released. Subsequently, about 68% of drugs within 3 h was released (87% release was for DCN dispersion in 3 h) and from the 4th h onward, the release rate was constant up to 86% of the drug was released. This result was further proved statistically by evaluating the data with the student t-test. A significant difference was found between the NLCs gel and plain DCN gel with a calculated p-value of <0.0001. From this study, it can be concluded that the formulation of NLCs provided a good and controlled release profile when compared to free drug. Further converting the dispersion into gel was more advantageous due to the smooth and sustained release profile than all the other three formulations.

For understanding the mechanism of drug release kinetics of drug from the optimized NLCs dispersion, the data was fitted into four different drug release kinetics models. For the optimized formulation, a linear relationship was found that fitted Higuchi's model as the correlation coefficient ( $r^2$  value) was highest (0.983) for this model. This fit indicated the diffusion mechanism of drug release from the NLC dispersion. For its confirmation, the data were fitted into the Korsmeyer Pappas model. This model explains the non-fickian nature of diffusion from the formulation. Since the exponential coefficient (value of  $n$ ) was 0.706 and it is known that if the value of 'n' lies between 0.5 and 1 the drug release mechanism tends to follow non-fickian diffusion and below 0.5 it follows fickian diffusion and above 1 it follows anomalous diffusion. Further, after incorporating the NLCs into the gel the drug release mechanism was changed to anomalous diffusion as the value of  $n$  was 1.023. However, the kinetic of drug release was following Higuchi's model. Anomalous diffusion indicated the release of a drug through more than one mechanism like diffusion and erosion. In the case of many gels, the drug release mainly occurred through swelling of the

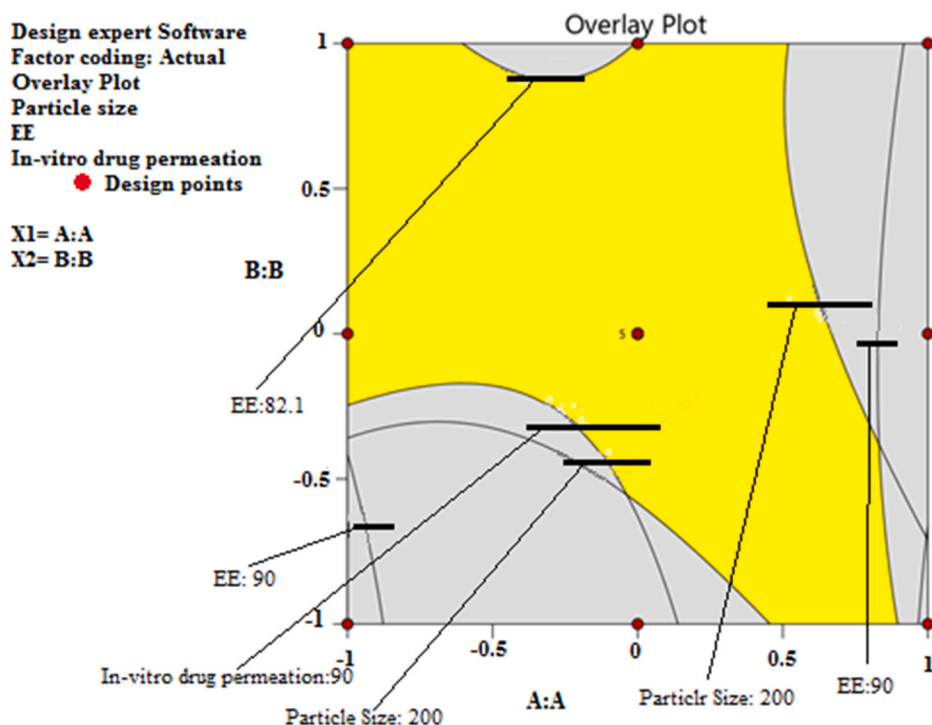


**Fig. 2.** Overlay plot of the responses  $Y_1$  (Particle Size),  $Y_2$  (% Entrapment efficiency) and  $Y_3$  (% Drug release ).

**Table 5**  
Optimized formulation.

Formulation	Factor A (Concentration of stearic acid in mg)	Factor B (Concentration of oleic acid in mg)	Responses						Desirability
			Particle Size (nm)		% Entrapment Efficiency		In-vitro Drug release at 24 h (%)		
			Predicted	Observed	Predicted	Observed	Predicted	Observed	
F 14	0.917	0.913	172.495	173.76	90.26	91.30	93.20	94.17	1

**Table 6**  
*In vitro* Drug Release Kinetics from optimized formulations.

Formulation	Zero order (R <sup>2</sup> )	First order (R <sup>2</sup> )	Higuchi's model (R <sup>2</sup> )	Koresmeyer-peppas model	
				(R <sup>2</sup> )	(n)
NLC dispersion	0.936	0.974	0.983	0.960	0.706
NLC loaded gel	0.922	0.947	0.983	0.954	1.023
Plain dispersion	0.983	0.886	0.942	0.899	0.421
Plain gel	0.972	0.916	0.976	0.832	0.543

### Comparative Ex- vivo Study

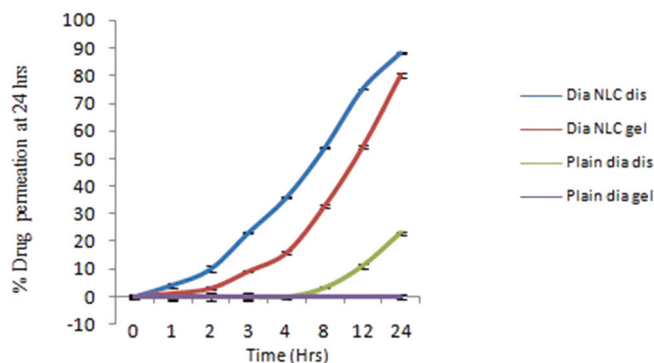


**Fig. 4.** Ex-vivo skin penetration studies for DCN-NLCs, DCN-NLCs gel, free DCN and DCN- gel formulations.

composition and particle size. These factors facilitated the enhanced permeation rate of the drug through the skin. Based on obtained results the prepared system can be considered a propitious carrier system for the topical delivery of the drug.

### 3.3.3. Drug loading

Drug loading capacity is one of the most important parameters of efficient nanoformulations. Drug loading was determined for the optimized formulation. It was found to be  $8.86 \pm 0.12\%$ . This data shows that the nanostructured lipid carriers possess a great amount of loading capacity for the drug molecule.

### 3.3.4. FTIR study

FTIR study was followed for determining the compatibility between DCN and other ingredients. FTIR spectra of pure drug DCN, its physical mixture with other ingredients, and lyophilized NLCs were given in Fig. 5(A) and (B), and (C). FTIR spectra of DCN show the peaks at  $1417.68 \text{ cm}^{-1}$ , (C=C stretching, aromatic),  $1668.43 \text{ cm}^{-1}$  (C=O stretching COOH),  $1026 \text{ cm}^{-1}$  (C-O stretching, ester), and  $1369.46 \text{ cm}^{-1}$  (OH bond stretching) as mentioned in Table 7. The FTIR spectrum of Diacerein (Fig. 2) also have shown the characteristic bands at  $3300 \text{ cm}^{-1}$  due to -OH broad stretching, and -COOH,  $3069.20 \text{ cm}^{-1}$  due to C-H, aromatic stretch,  $2935 \text{ cm}^{-1}$  due to C-H, symmetric aliphatic stretch  $1764.56 \text{ cm}^{-1}$  due to C=O, ester,  $1677 \text{ cm}^{-1}$  due to C=O stretch of COOH,  $1593.20 \text{ cm}^{-1}$  due to C=C aromatic stretch,  $1450.47 \text{ cm}^{-1}$  due to C-O stretch of COOH,  $1024.21 \text{ cm}^{-1}$  due to C-O stretch of ester,  $760.43 \text{ cm}^{-1}$  due to m-substituted benzene and  $703.02 \text{ cm}^{-1}$  due to benzene. These characteristic peaks are relative to the literature. This relevance denotes the drug's purity and absence of any kind of impurity. These peaks are characteristics of DCN. Similar peaks were observed in the FTIR spectra of the physical mixture and lyophilized NLCs also. The drug and additives interaction can be found as additional peaks in the FTIR spectra of formulations. The characteristic m-substituted peak at  $760 \text{ cm}^{-1}$  of Diacerein was also found in the physical mixture and lyophilized formulation. All these points indicate the compatibility of the drug with its ingredients.

### Comparative In- vitro Study

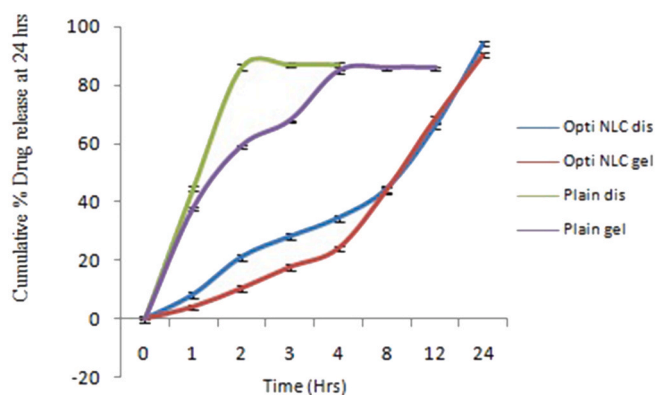


**Fig. 3.** *In vitro* drug release study for DCN-NLCs dispersion, DCN-NLCs gel, free DCN and DCN loaded gel.

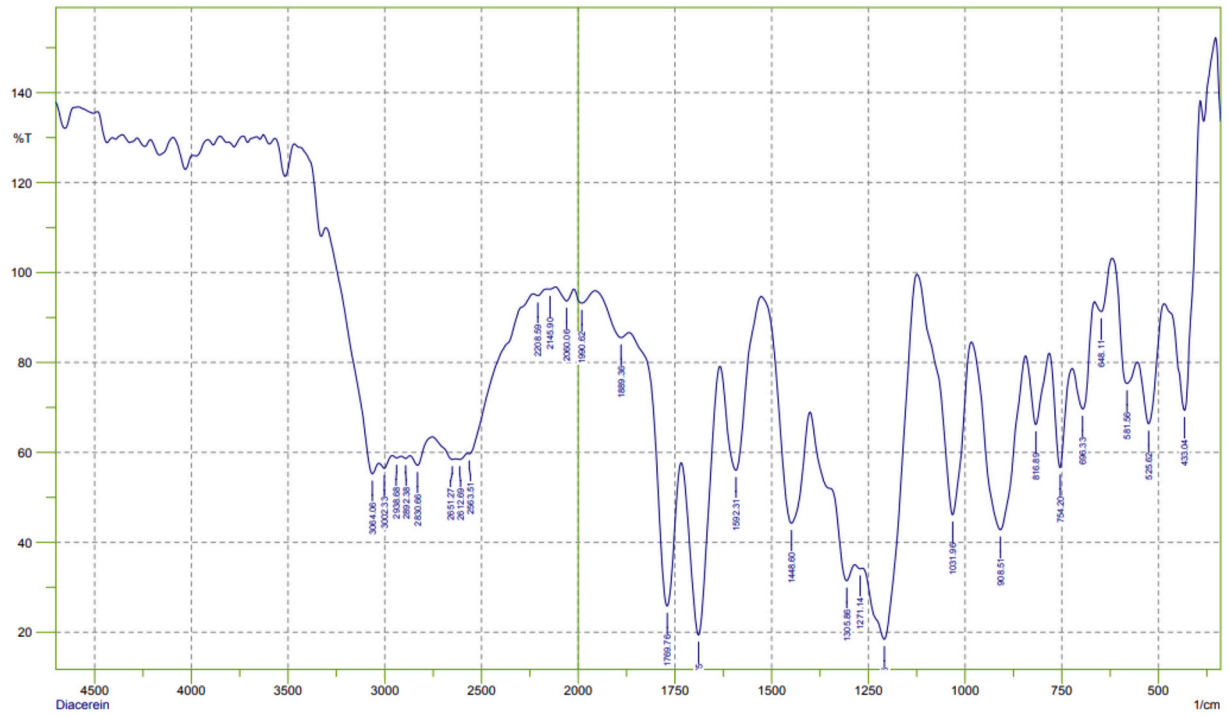
gel followed by diffusion. This change in release kinetics may be due to the fact of the 3D gel structure which causes the release through the fickian diffusion process (Ramalingam et al., 2013).

### 3.3.2. Ex-vivo skin permeation study

The ex-vivo permeation study was performed to explain the release pattern through the abdominal skin of albino rats. The formulations under study were NLC dispersion, NLC gel, plain DCN dispersion, and plain DCN gel. A comparative graph for the cumulative % drug permeation study of the above-mentioned formulations is given in Fig. 4. It is noticed that drug permeation was gradually increased up to 88.25% at 24 h for NLC dispersion. The drug permeation rate was low in case of NLCs gel in initial hours which was then gradually enhanced up to 80.13% as time passed. The drug permeation was completely absent initially in case of plain DCN gel and plain DCN dispersion. The drug permeation for the plain DCN dispersion was initiated after 8hr of the study and then it was increased sluggishly up to 23.15%. But in case of plain DCN gel, there was no sign of drug release during the whole study. So, the results showed that the rate of permeation was significantly ( $p < 0.001$ ) greater, sustained, and complete in case of NLC dispersion and NLC gel as compared to plain drug dispersion and plain gel. However, the total % drug permeation was decreased when compared to in vitro drug release study. This result can be explained based on formulation



A



B

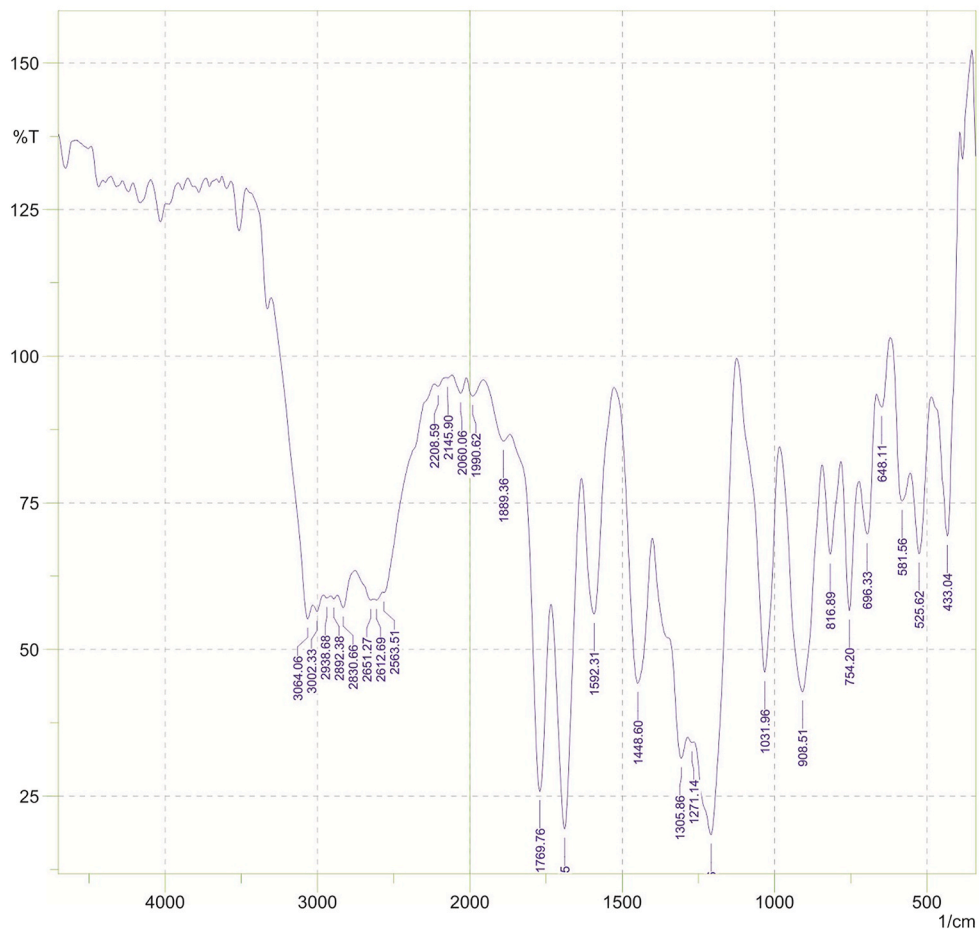


Fig. 5. FTIR spectra (A) Pure DCN (B) Physical mixture (C) Lyophilized NLCs.



C

SHIMADZU

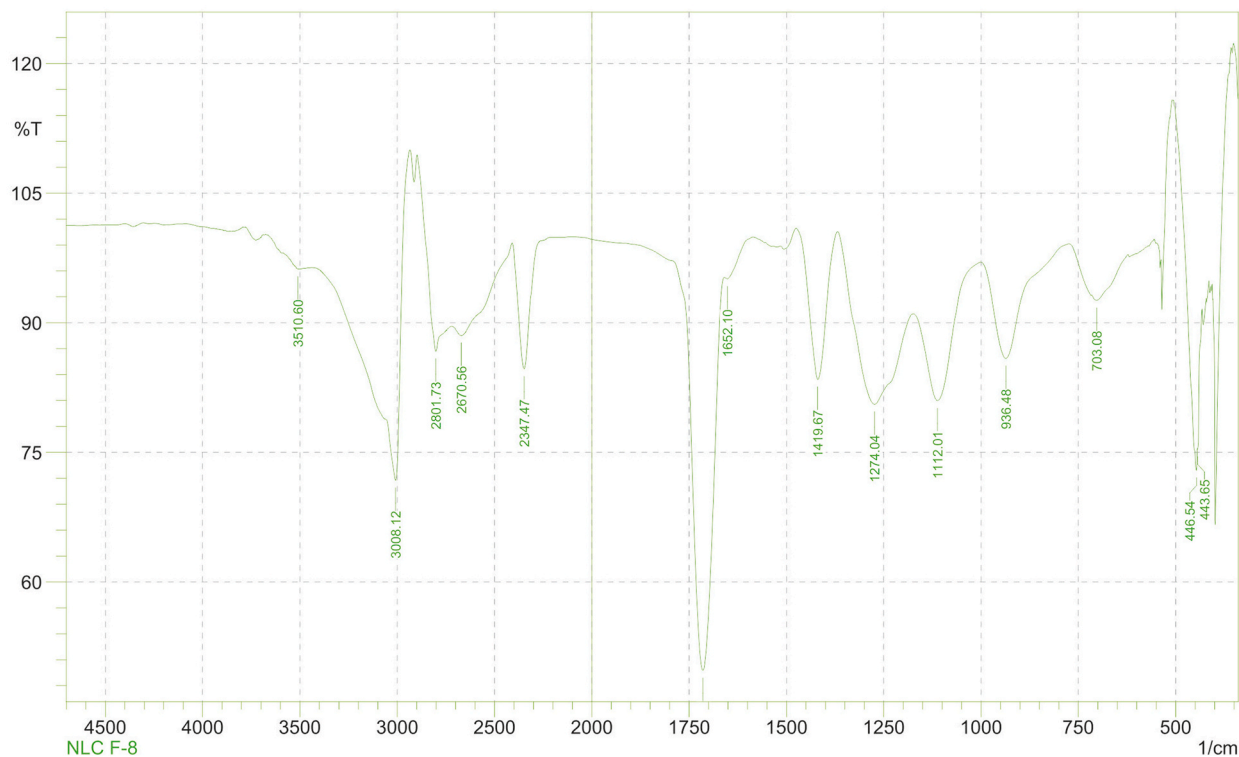


Fig. 5. (continued).

Table 7

Some characteristic infrared absorption regions.

S. No.	Bond	Frequency (cm <sup>-1</sup> )
1.	C=C stretching	1417.68
2.	C=O stretching	1668.43
3.	C-O stretching	1026.13
4.	O-H stretching	1369.46

### 3.3.5. XRD study

This technique was used to gather information about the crystalline or amorphous nature of the powdered drug and the lyophilized NLC formulation. The high-intensity sharp peaks of the diffractogram denote the crystalline behavior of the powder while the low-intensity peaks indicate the amorphous nature. The XRD pattern of DCN has shown sharp and high-intensity peaks on the 2 theta scale at 10.74, 10.72, and 17.60, 17.65, 17.62, 17.54, etc (Fig. 6). These peaks are characteristics of pure DCN and show its crystalline nature. The lyophilized NLC showed high-intensity peaks only at about 21.77, 21.75, and 21.69 angles. These high-intensity peaks found in the diffractogram may be due to the minor existence of the drug at the outer layer of the lipid matrix. The decreased intensities found in the formulation denote the reduction of crystalline behavior and increased amorphous nature. In other words, the presence of a combination of low and high-intensity peaks explains the imperfect lattice structure of the formulation. Such imperfection in the structure provides greater space for the entrapment of the drug in the formulation. The diffractogram shows the increased solubility of the poorly soluble drug.

### 3.3.6. Thermal study

DSC study provides information about the phase transition and the

effect of thermal changes on the physical state of the sample. The DSC study also explains different types of changes in the properties of the drug after the drug's loading in to the carrier system. Differential scanning calorimeter model DSC 404F3 Pegasus by NETZSCH was used for the analysis. The pure drug DCN, lipid stearic acid, their physical mixture, and the lyophilized NLCs sample were analyzed by the instrument. Various DSC thermograms are shown in Fig. 7. A sharp peak at 256 °C has been found in the DSC thermogram of pure drug denoting its melting point. Stearic acid has shown its melting point at 69 °C. The physical mixture and lyophilized NLC sample have also shown a sharp and clear peak of stearic acid while the peak of the drug disappeared in both of these cases. The disappearance of sharp peaks of the drug in the thermograms might be accredited to the complete molecular solubilization of drugs in lipids. The results are correlated with the literature reported (Pokharkar et al., 2017; Wavikar and Vavia, 2015).

### 3.3.7. Surface morphology study by HRTEM

The transmission electron micrograph of the optimized formulation is shown in Fig. 8. The external surface morphological study revealed that the prepared NLCs are well-defined spherical and the size observed is well correlated with observations of the zeta sizer. Also, the micrograph has shown that the particles are in discrete positions and there was not any sign of agglomeration. The optimized formulation was selected for further study.

### 3.3.8. Characterization of gel

The optimized formulation of NLCs was converted into the gel with Carbopol 940. Various characterization parameters were followed for determining the gel's quality. The data obtained are summarized in Table 8. The gel prepared was found homogeneous, properly spreadable, and possesses pH, viscosity, and drug content in a good range.

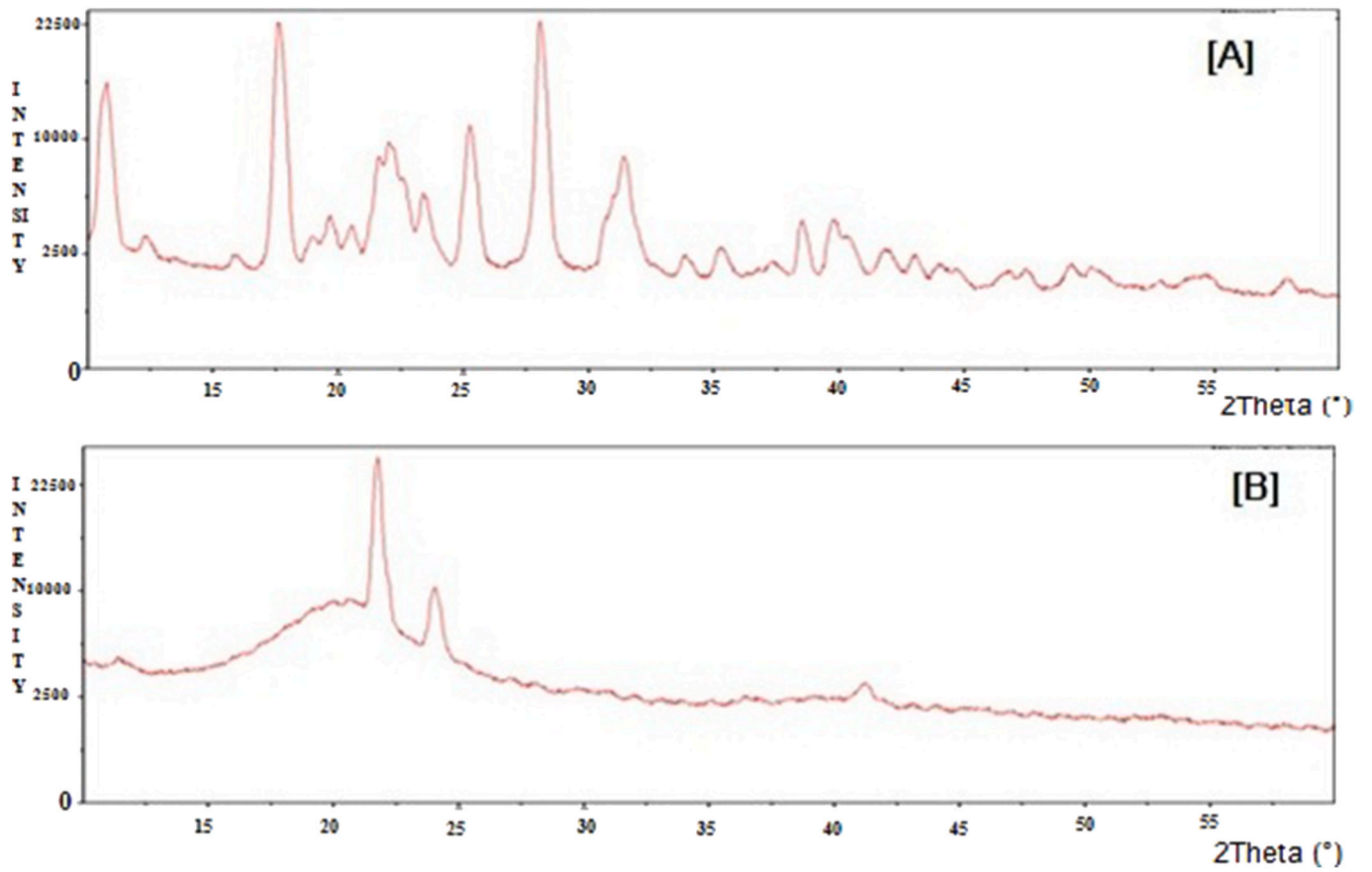


Fig. 6. X ray diffractogram (A) Pure drug (B) Lyophilized NLCs.

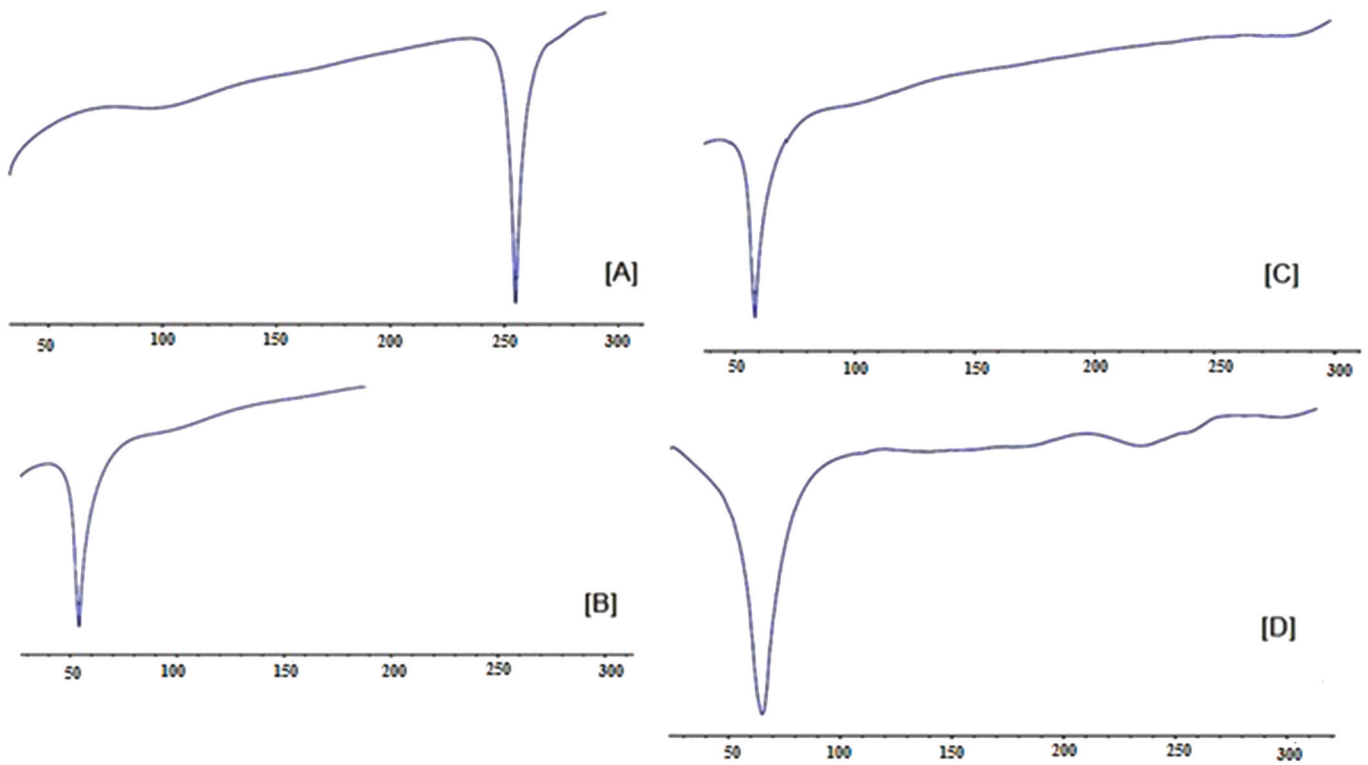


Fig. 7. DSC thermograms of (A) Pure drug DCN (B) Stearic acid (C) Physical Mixture (D) Lyophilized NLCs.

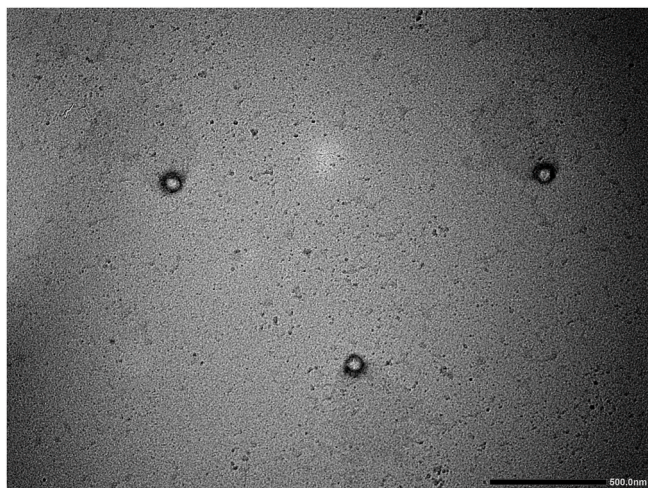


Fig. 8. High Resolution Transmission Electron Micrograph of optimized DCN loaded NLCs.

Table: 8  
Characterization of DCN-NLC loaded Gel.

S. No.	Parameter	Observation
1.	Homogeneity	Good, Homogeneous
2.	pH	6.4 ± 0.75
3.	Viscosity	16,000 ± 0.83 cps
4.	Spreadability	16.85 ± 0.46 gm cm/sec
5.	Drug Content	88.96 ± 1.12%

### 3.3.9. Stability study

The optimized formulation was put on refrigerated, general, and accelerated stability study. The physical changes in formulation, particle size, and % EE were measured after the storage. No significant change has been observed in optimized formulation after storage in all three storage conditions. The particle size was increased slightly and % EE was decreased after 90 days of storage in all the cases. But these changes are not that significant to affect the formulation efficiency. Table 9 shows the changes observed after storage.

## 4. Conclusion

This study explains the development and optimization of DCN-loaded NLC for its topical application. DCN loaded NLC formulation was successfully prepared by the hot homogenization method and optimized by face centered central composite design. The optimized formulation was amorphous, spherical shaped and possessed satisfactory entrapment efficiency, particle size, and sustained drug release. The DCN loaded NLC formulation incorporated gel was homogeneous and possessed good spreadability, viscosity, and suitable pH condition for topical applications. The chosen method was good, cost-effective, and less time-consuming. Further, the NLC gel displayed sustained drug release through the in-vitro model that was further approved by an ex-vivo skin permeation study. Therefore, it can be concluded that DCN loaded nanostructured lipid carriers may show desired topical penetration of the drug when if tested in animal experiments. Future pre-clinical studies are required for establishing this fact in experimental animal models.

### Animal ethical committee permission

For performing an ex-vivo permeation study, a due permission was taken from the Institutional Animal Ethical Committee of Columbia Institute of Pharmacy, Raipur, Chhattisgarh, India. The registration

Table: 9  
Stability study data.

Parameters of study	Storage conditions		
	(4±2 °C)	25±2 °C/60 ± 5% RH	40 ± 2 °C and 75 ± 5% RH
Physical appearance	No change	No change	No change
Particle Size	201.45 ± 0.66 nm	203.09 ± 1.47 nm	214.23 ± 0.34 nm
% EE	86.4 ± 0.56%	85.7 ± 0.49%	79.5 ± 1.34%

number is CIP/IAEC/2018/125. The guidelines of CPCSEA were duly followed during the study.

## Data and materials

The data supporting the findings of the article is available within the article.

## Funding

No funding agency was involved.

## Declaration of competing interest

No potential conflict of interest was reported by the author.

## References

- Agrawal, M., Saraf, S., Pradhan, M., Patel, R. J., Singhvi, G., & Alexander, A. (2021). Design and optimization of curcumin loaded nano lipid carrier system using Box-Behnken design. *Biomedicine & Pharmacotherapy*, 141, 1119-19.
- Aliaa, N., ElMeshad, I., & Ibrahim, M. T. (2011). Transdermal delivery of an anti-cancer drug via W/O emulsions based on alkyl polyglycosides and lecithin: Design, characterization, and in vivo evaluation of the possible irritation potential in rats. *AAPS PharmSciTech*, 12(1), 1-9.
- Alsarra, I. A., Bosela, A. A., Ahmed, S. M., & Mahrous, G. M. (2005). Proniosomes as a drug carrier for transdermal delivery of ketorolac. *European Journal of Pharmaceutics and Biopharmaceutics*, 59, 485-490.
- Giannellini, V., Salvatore, F., Bartolucci, G., Coran, S. A., & Alberti, M. B. (2005). A validated HPLC stability-indicating method for the determination of diacerein in bulk drug substance. *Journal of Pharmacy Biomedicine Analytical*, 39, 776.
- Gupta, R. R., Jain, S. K., & Varshney, M. (2005). AOT water-in-oil microemulsions as a penetration enhancer in transdermal drug delivery of 5-fluorouracil. *Colloids and Surfaces B*, 41(1), 25-32.
- Gupta, A., Singh, S., Kotla, N. G., & Webster, T. J. (2014). Formulation and evaluation of a topical niosomal gel containing a combination of benzoyl peroxide and tretinoin for antiacne activity. *International Journal of Nanomedicine*, 10, 171-182.
- Jadon, P. S., Gajbhiye, V., Jadon, R. S., Gajbhiye, K. R., & Ganesh, N. (2009). Enhanced oral bioavailability of griseofulvin via niosomes. *AAPS PharmSciTech*, 10, 1186-1192.
- Jain, K., Sood, S., & Gowthamarajan, K. (2015). Optimization of artemether-loaded NLC for intranasal delivery using central composite design. *Drug Delivery*, 22(7), 940-954.
- Kesharwani, D., Paliwal, R., Satapathy, T., & Paul, S. D. (2019). Rheumatoid arthritis: An updated overview of latest therapy and drug delivery. *J. pharmacopunct.*, 22(4), 210-225.
- Khandavilli, S., & Panchagnula, R. (2007). Nanoemulsions as versatile formulations for paclitaxel delivery: Peroral and dermal delivery studies in rats. *Journal of Investigative Dermatology*, 127(1), 154-162.
- Liu, F., Xiao, Y. Y., Ping, Q. N., & Yang, C. (2009). Water in oil microemulsions for transdermal delivery of fluorouracil. *Yaoxue Xuebao*, 44(5), 540-547.
- Lunter, D., & Daniels, R. (2013). In vitro skin permeation and penetration of nonivamide from novel fi lm-forming emulsions. *Skin Pharmacology and Physiology*, 26, 139-146.
- Mira, E. G., Egeaa, M. A., Garciaa, M. L., & Souto, E. B. (2010). Design and ocular tolerance of flurbiprofen loaded ultra sound engineered NLC. *Colloids Surg. B. Biointerfaces*, 81(2), 412-421.
- Naglakshmi, S., Shanmuganathan, S., Sandhya, K., & Anbarasan, B. (2018). Design, development and characterization of nano structured lipid carrier for topical delivery of aceclofenac. *Ind. J. Pharm. Edu. Res.*, 52(4), 581-586.
- Nguyen, M., Yaron, M., Haraoui, B., Cohen, P., Nahir, M. A., Choquette, D., Wigler, I., Rosner, I. A., & Beaulieu, A. D. (1994). Diacerein in the treatment of osteoarthritis of the hip. *Arthritis & Rheumatism*, 37(4), 529-536.
- Nimila, I. C., Balan, P., Kumar, D. Y., & Rajasekar, S. (2010). Simultaneous estimation of diacerein and aceclofenac in bulk and pharmaceutical dosage form by uv spectroscopy method. *Int. J. Pharm. Tech. Res.*, 2, 2313-2318.

- Paliwal, R., Paliwal, S. R., Kenwat, R., Kurmi, B. D., & Sahu, M. K. (2020). Solid lipid nanoparticles: A review on recent perspectives and patents. *Expert Opinion on Therapeutic Patents*, 30(3), 179–194.
- Patel, N. S., Nandurbarkar, V. P., Patel, A. J., & Patel, S. G. (2014). Simultaneous spectrophotometric determination of celecoxib and diacerein in bulk and capsule by absorption correction method and chemometric methods. *Spectrochim. Acta A Mol. Biomol. Spectrosc.*, 125, 46–52.
- Pelletier J.P., et al., Efficacy and safety of diacerein in osteoarthritis of the knee: A double-blind, placebo-controlled trial. The diacerein study group, *Arthritis & Rheumatism* ;43(10):2339-2348.
- Pokharkar, V., Patil-Gadhe, A., & Palla, P. (2017). Efavirenz loaded nanostructured lipid carrier engineered for brain targeting through intranasal route: In-vivo pharmacokinetic and toxicity study. *Biomedicine & Pharmacotherapy*, 94, 150–164.
- Rai, V. S. P., Paliwal, S., Gupta, R., Khatri, P. N., Goyal, K., & Vaidya, A. K. B. (2008). Solid lipid nanoparticles (SLNs) as a rising tool in drug delivery science: One step up in nanotechnology. *Current Nanoscience*, 4(1), 30–44.
- Ramalingam, N., Natesan, Dhandayuthapani, B., Perumal, P., Balasundaram, J., & Natesan, S. (2013). Design and characterization of ofloxaciniosomes. *Pakistan journal of pharmaceutical sciences*, 26, 1089–1096.
- Roberts, M. S., Lai, P. M., Cross, S. E., & Yoshida, N. H. (1997). *Mechanism of transdermal drug delivery*. Marcel Dekker, 291–249.
- Schwartz, J. B., O'connor, R. E., & Schnaare, R. L. (2007). Optimization technique in pharmaceutical formulation and processing. *Drugs and the Pharmaceutical Sciences*, 72, 607–627.
- Souto, E. B., Mehnert, W., & Müller, R. H. (2006). Polymorphic behavior of Compritol888 ATO as bulk lipid and as SLN and NLC. *Journal of Microencapsulation*, 23, 417–433.
- Tiwari, S., Mistry, P., & Patel, V. (2014). SLNs based on co-processed lipids for topical delivery of terbinafine hydrochloride. *J Pharm Drug Dev*, 1(6), 604.
- Tran, T. H., Ramasamy, T., Cho, H. J., Kim, Y. I., Poudel, B. K., Choi, H. G., Yong, C. S., & Kim, J. O. (2014). Formulation and optimization of raloxifene-loaded solid lipid nanoparticles to enhance oral bioavailability. *Journal of Nanoscience and Nanotechnology*, 14(7), 4820–4831.
- Wavikar, P. R., & Vavia, P. R. (2015). Rivastigmine-loaded in situ gelling nanostructured lipid carriers for nose to brain delivery. *Journal of Liposome Research*, 25(2), 141–149.
- Zhang, Q., Jiang, X., & Jiang, W. (2004). Preparation of nimodipineloading microemulsion for intranasal delivery and evaluation on the targeting efficiency to the brain. *International Journal of Pharmacy*, 275(1–2), 85–96.